

NUMERICAL INVESTIGATION OF A SMD VISCOPLASTIC MATERIAL THROUGH A 4:1 ABRUPT CONTRACTION

Graziela G. Ramos, graziela@ct.ufes.br

Edson J. Soares, edson@ct.ufes.br

Grupo de Escoamento de Fluidos Complexos-LFTC-Department of Mechanical Engineering, Universidade Federal do Espírito Santo, Avenida Fernando Ferrari, 514, Goiabeiras, 29075-910, ES, Brazil

Roney L. Thompson, rthompson@mec.uff.br

Grupo de Escoamento de Fluidos Complexos-LMTA-PGMEC, Department of Mechanical Engineering, Universidade Federal Fluminense, Rua Passo da Patria 156, 24210-240, Niteroi, RJ, Brasil

Abstract. *Viscoplastic materials are commonly found in a variety of industrial processes, like in the food industry, the cosmetic industry, painting industry, petroleum industry and so on. Besides that, in almost all of the processes in these industries, this kind of fluid is submitted to a change on the diameter of the tube flow. Therefore, the abrupt contraction is a classical geometry to test new material models. A Galerkin Finite Element Method is used to investigate the performance of a SMD (Souza Mendes and Dutra, 2004) viscoplastic material through a 4:1 abrupt contraction. The concept, widely used in the literature, of the yield surface, closely related to a Bingham material, is replaced by an yield zone, an intermediate transition region where the flow occurs, but at stress levels very close to the yield stress. An open issue is related to the best way of defining the boundaries of this yield zone, since it does not seem possible to define it in a non-subjective manner. If the criterion is stress-based or deformation-rate based is another open issue that we try to address. The influence of dimensionless parameters like the Jump number and an equivalent to the Bingham number on the size of the yield zone and on the pressure loss of the contraction are investigated.*

Keywords: *Viscoplastic material, abrupt contraction flow, finite element method*

1. INTRODUCTION

There is a large variety of materials that have a viscoplastic-like behavior. Conceptually, a viscoplastic material is a material that possesses a yield-stress, τ_0 , a stress limit below which the material does not flow. The first model that could predict this kind of behavior was proposed by Bingham (1922) as

$$\begin{cases} \eta = \frac{\tau_0}{\dot{\gamma}} + \mu_p & \text{se } \tau \geq \tau_0 \\ \dot{\gamma} = 0 & \text{se } \tau < \tau_0 \end{cases} \quad (1)$$

where $\tau = \sqrt{\frac{1}{2}\boldsymbol{\tau} \cdot \boldsymbol{\tau}}$ and $\dot{\gamma} = \sqrt{\frac{1}{2}\dot{\boldsymbol{\gamma}} \cdot \dot{\boldsymbol{\gamma}}}$ are the norms of the deviatoric part of the stress tensor, $\boldsymbol{\tau} = \mathbf{T} + p\mathbf{1}$, and the rate-of-deformation tensor, $\dot{\boldsymbol{\gamma}} = \nabla\mathbf{v} + \nabla^T\mathbf{v}$, respectively. \mathbf{T} is the total stress tensor, p is the mechanical pressure, $\mathbf{1}$ is the identity tensor, $\nabla\mathbf{v}$ is the velocity gradient and the superscript T indicates the transpose of the tensor. The quantity η is the viscosity function associated to the Generalized Newtonian Liquid equation, $\boldsymbol{\tau} = \eta\dot{\boldsymbol{\gamma}}$.

For the representation of a material that behaves like a power-law fluid after the achievement of the yield stress, the model of Hershell-Buckley was proposed as

$$\begin{cases} \eta = \frac{\tau_0}{\dot{\gamma}} + k\dot{\gamma}^{n-1} & \text{se } \tau \geq \tau_0 \\ \dot{\gamma} = 0 & \text{se } \tau < \tau_0 \end{cases} \quad (2)$$

The relation $\tau \times \dot{\gamma}$, presented in Eqs.(1) and (2), is not a function for every value of $\dot{\gamma}$. When $\dot{\gamma} = 0$, there are an infinity of values, in the interval $[0, \tau_0]$ that τ can assume and the viscosity is infinite. In order to represent the Bingham model numerically, it is common to use a bi-viscosity function using a very high viscosity value for low values of the shear rate.

However, there is a controversy in the literature, with respect to the class of viscoplastic materials. With the improvement of the accuracy of the rheometric measurements, some authors advocated that, strictly speaking, there are no materials with yield stresses. In other words, these materials would flow with any finite level of stress. The alternative explanation for the behavior of such materials that seem to have an yield stress is that, in fact, there is a huge decrease in viscosity for a very small change in the shear rate (or stress). In other words, instead of not flowing, this alternative approach considers that the material has a very high viscosity for low values of shear rate. When stress increases, there would be a rearrangement of the material structure that would lead to a decrease on the viscosity. An interesting review on the subject was made by Barnes (1999). Although the existence or non-existence of the yield-stress is important in the philosophical point-of-view, as pointed by ? the relevant issue is related to how we model the material for engineering purposes. Therefore, the yield stress can be considered "an engineering reality".

A viscoplastic model widely used in the literature as an alternative, for the bi-viscosity model, in trying to capture the behavior of a Bingham material is the one proposed by Papanastasiou (1987) given by

$$\eta = \frac{\tau_0}{\dot{\gamma}} [1 - \exp(-m\dot{\gamma})] + \mu_p, \quad (3)$$

transforming the stress-strain relation into a function. The quantity m is generally called a regularization parameter. As $m \rightarrow \infty$ Papanastasiou's model approaches Bingham's one. In the manner it was conceived, i.e. to reproduce Bingham-like behavior, m has to have a high value. The literature recommends a dimensionless form $m^* = 1000$ (You et al., 2008). However, from the non-existence-of-yield-stress perspective, we can notice that

$$\eta_0 \equiv \lim_{\dot{\gamma} \rightarrow 0} \eta = \tau_0 m + \mu_p \Rightarrow m = \frac{\eta_0 - \mu_p}{\tau_0} \quad (4)$$

giving to m a physical interpretation through its relation with η_0 , the high viscosity level at low shear rates. Papanastasiou's model can be rewritten as

$$\eta = \left[1 - \exp\left(-\frac{\eta_0 - \mu_p}{\tau_0} \dot{\gamma}\right) \right] \frac{\tau_0}{\dot{\gamma}} + \mu_p, \quad (5)$$

Although there is a quantity in the model represented by the symbol τ_0 (or τ_y), it is worth noticing that, in fact, there is not a true yield stress, since the material flows with a level of stress below this value. This quantity can be interpreted as an apparent yield stress. Therefore, this model is more aligned to the second way of thinking. Papanastasiou's model was used by several authors Sousa et al. (2007), Dimakopoulos and Tsamopoulos (2003), You et al. (2008), among others.

The analogous adjustment, with a regularization parameter, of the Hershell-Bulckley commonly used in the literature is

$$\eta = \frac{\tau_0}{\dot{\gamma}} [1 - \exp(-m\dot{\gamma})] + k\dot{\gamma}^{n-1}. \quad (6)$$

However, there is a great difference between the adjusted Hershell-Bulckley model and the adjusted Bingham model (Papanastasiou), in the $\dot{\gamma} \rightarrow 0$ limit, when the fluid presents shear-thinning behavior ($n < 1$). Although the inclusion of the regularization parameter in the case of the Hershell-Bulckley model do transform the stress-strain relation into a function, it does not present a bounded value for $\eta_0 = \lim_{\dot{\gamma} \rightarrow 0} \eta$. This result motivate de Souza Mendes and Dutra (2005) to propose another equation for the stress-strain relation, in consonance to the idea of the existence of a finite high viscosity value for low shear-rates, as

$$\eta = [1 - \exp(-m\dot{\gamma})] \left(\frac{\tau_0}{\dot{\gamma}} + k\dot{\gamma}^{n-1} \right) \quad (7)$$

It is easy to show that $\eta_0 = \lim_{\dot{\gamma} \rightarrow 0} \eta = m\tau_0$, and thus, $m = \frac{\eta_0}{\tau_0}$ is a characteristic time of the material with a very clear physical interpretation. The final form of the Souza Mendes and Dutra equation is

$$\eta = \left[1 - \exp\left(-\frac{\eta_0 \dot{\gamma}}{\tau_0}\right) \right] \left(\frac{\tau_0}{\dot{\gamma}} + k\dot{\gamma}^{n-1} \right) \quad (8)$$

2. PHYSICAL FORMULATION

2.1 Governing equations and boundary conditions

The problem chose to evaluate the performance of the SMD equation is the 4:1 abrupt contraction. The scheme of this problem is depicted in Fig. 1.

The velocity and pressure fields are defined by the governing equations that impose conservation of mass and momentum for a noninertial incompressible fluid, together with the appropriate boundary conditions.

$$\frac{1}{r} \frac{\partial}{\partial r}(rv) + \frac{\partial u}{\partial r} = 0 \quad (9)$$

$$\frac{1}{r} \frac{\partial}{\partial r}(rT_{(xr)}) + \frac{\partial}{\partial x}(T_{(xx)}) = 0 \quad (10)$$

$$\frac{1}{r} \frac{\partial}{\partial r}(rT_{(rr)}) - \frac{T_{(\theta\theta)}}{r} + \frac{\partial}{\partial x}(T_{(rx)}) = 0 \quad (11)$$

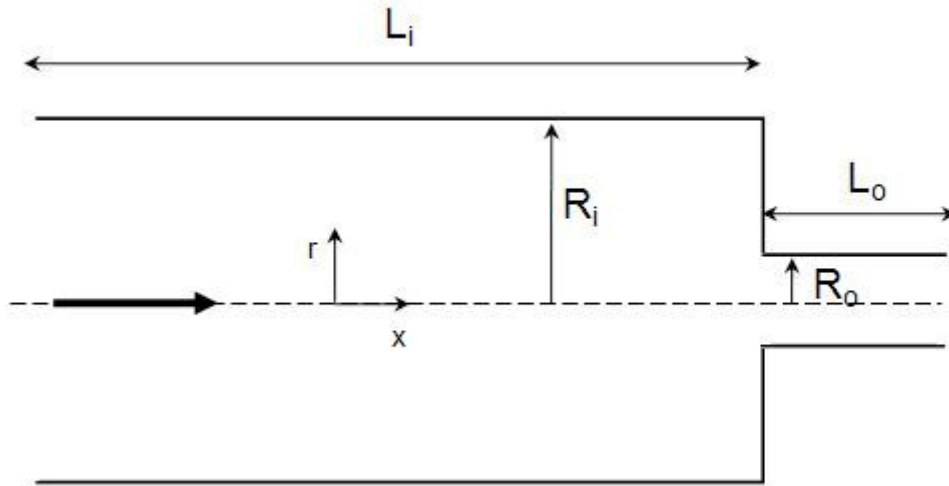


Figure 1. 4:1 abrupt contraction

Where u and v are respectively the axial and radial components of the velocity field \mathbf{u} and the quantities T_{xx} , T_{xr} , T_{rx} , T_{rr} and $T_{\theta\theta}$ are the components of the stress tensor \mathbf{T} .

The boundary conditions are described next. At the inlet and outlet, the flow is considered fully-developed and the pressure is imposed.

Along the symmetry axis both the shear stress and the radial velocity vanish

The no-slip and impermeability conditions are imposed along the walls

2.2 Features of the SMD equation

For a better understanding of the main features of the SMD equation, we analyze in detail its main aspects of the model. For a deeper comprehension, the reader is referred to the works ?. The SMD equation can be written as a stress function of the shear-rate,

$$\tau = \left[1 - \exp\left(-\frac{\eta_0 \dot{\gamma}}{\tau_0}\right) \right] (\tau_0 + k \dot{\gamma}^n) \quad (12)$$

As shown in Fig. 2, the stress function can be roughly divided into three parts. The first one, for low values of the shear-rate, where stresses are below the “yield-stress”, is a Newtonian region with a viscosity plateau of value η_0 . The intermediate part is defined by a region where the stress has achieved a critical value, τ_0 , and remains *close* to this value for a certain range of shear-rate. In the third and last part the material behaves as a power-law fluid of parameters k , n .

The characteristic deformation rate is chosen, in accordance to de Souza Mendes (2007), as the deformation rate that the power-law region for a stress intensity of τ_0 . Therefore,

$$\dot{\gamma}_c = \left(\frac{\tau_0}{\kappa} \right)^{\frac{1}{n}} \quad (13)$$

It can be shown that, in the correspondent stress for this value of the deformation rate is $\tau = 2\tau_0$. The so-called Jump number is a dimensionless number that measures the relative range the deformation rate assume when the stress intensity is close to τ_0 . It is defined as

$$J = \frac{\dot{\gamma}_c - \dot{\gamma}_0}{\dot{\gamma}_0} = \frac{\dot{\gamma}_c}{\dot{\gamma}_0} - 1 \quad (14)$$

3. NUMERICAL FORMULATION

3.1 Solution of the equation system by Galerkin / Finite Element Methods

The Finite Element method is used with a Galerkin formulation to solve the differential equations that govern the problem. Biquadratic basis functions ϕ_j are used to represent the velocity and nodal coordinates, while linear discontinuous functions χ_j are employed to expand the pressure field. The velocity and pressure are represented in terms of appropriate basis functions

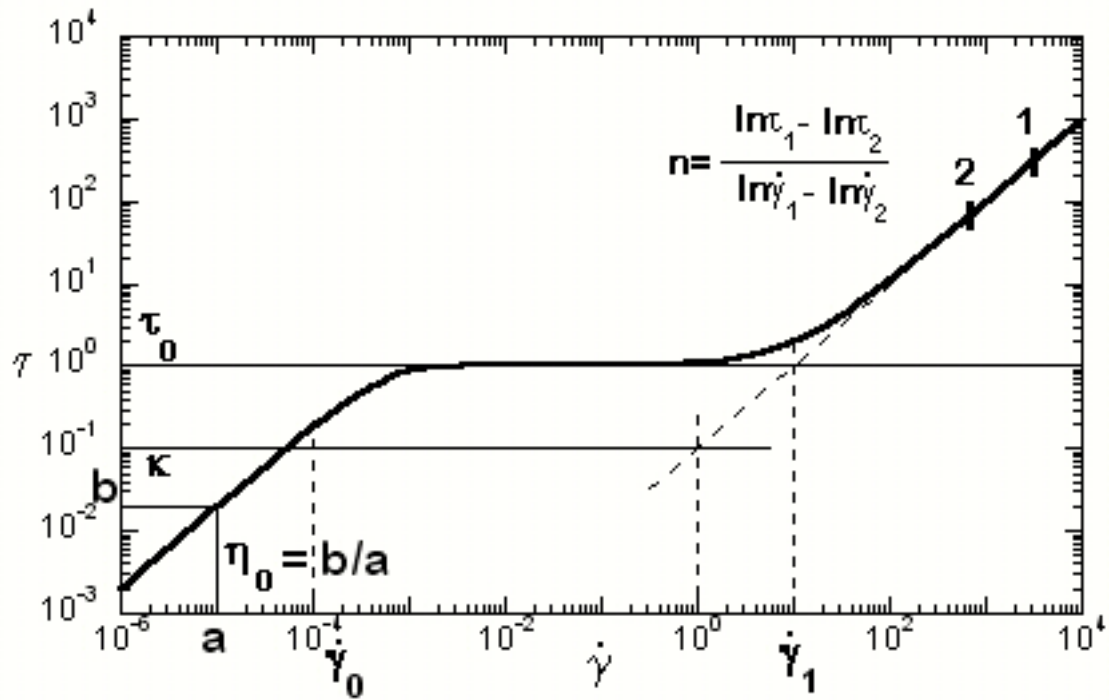


Figure 2. Deformation rate for a fixed value of the Jump Number, $J = 2500$, and different values of power-law index.

$$u = \sum_{j=1}^n U_j \phi_j \quad ; \quad v = \sum_{j=1}^n V_j \phi_j \quad ; \quad p = \sum_{j=1}^m P_j \chi_j \quad ; \quad (15)$$

The coefficients of the expansions are the unknown of the problem

$$\underline{c} = [U_j \quad V_j \quad P_j]^T$$

The corresponding weighted residuals of the Galerkin method related to conservation of momentum, mass and mesh generation are:

$$R_c^i = \int_{\bar{\Omega}} \left[\frac{1}{r} \frac{\partial}{\partial r} (rv) + \frac{\partial u}{\partial x} \right] \chi_i r ||J|| d\bar{\Omega} \quad (16)$$

$$R_{mx}^i = \int_{\bar{\Omega}} \left[\frac{\partial \phi_i}{\partial x} T_{(xx)} + \frac{\partial \phi_i}{\partial r} T_{(xr)} \right] r ||J|| d\bar{\Omega} - \int_{\bar{\Gamma}} \mathbf{e}_x \cdot (\mathbf{n} \cdot \mathbf{T}) \phi_i r \frac{d\Gamma}{d\bar{\Gamma}} d\bar{\Gamma} \quad (17)$$

$$R_{mr}^i = \int_{\bar{\Omega}} \left[\frac{\partial \phi_i}{\partial x} T_{(xr)} + \frac{\partial \phi_i}{\partial r} T_{(rr)} + \frac{\phi}{r} T_{(\theta\theta)} \right] r ||J|| d\bar{\Omega} - \int_{\bar{\Gamma}} \mathbf{e}_r \cdot (\mathbf{n} \cdot \mathbf{T}) \phi_i r \frac{d\Gamma}{d\bar{\Gamma}} d\bar{\Gamma} \quad (18)$$

3.2 Solution of the non-linear system of algebraic equation by Newton's Method

As indicated above, the system of partial differential equations, and boundary conditions is reduced to a set of simultaneous algebraic equations for the coefficients of the basis functions of all the fields. This set is non-linear and sparse. It is solved by Newton's method. The linear system of equations at each Newton iteration was solved using a frontal solver.

The mesh used to solve the present problem is depicted in Fig. 3. It has 3801 nodes with 25404 degrees of freedom.

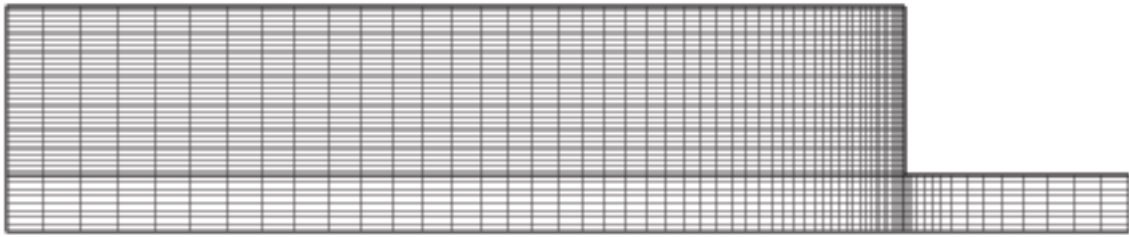


Figure 3. Deformation rate for a fixed value of the Jump Number, $J = 2500$, and different values of power-law index.

4. RESULTS

On the top of Fig. 4 is the plot of the stress intensity as a function of the deformation rate for a fixed Jump number, $J = 2500$, and different values of the power-law index. The fields of stress intensity for the different values the power-law index are shown below. On the left, there are only three levels of intensity: below τ_0 , between τ_0 and $2\tau_0$, and above $2\tau_0$.

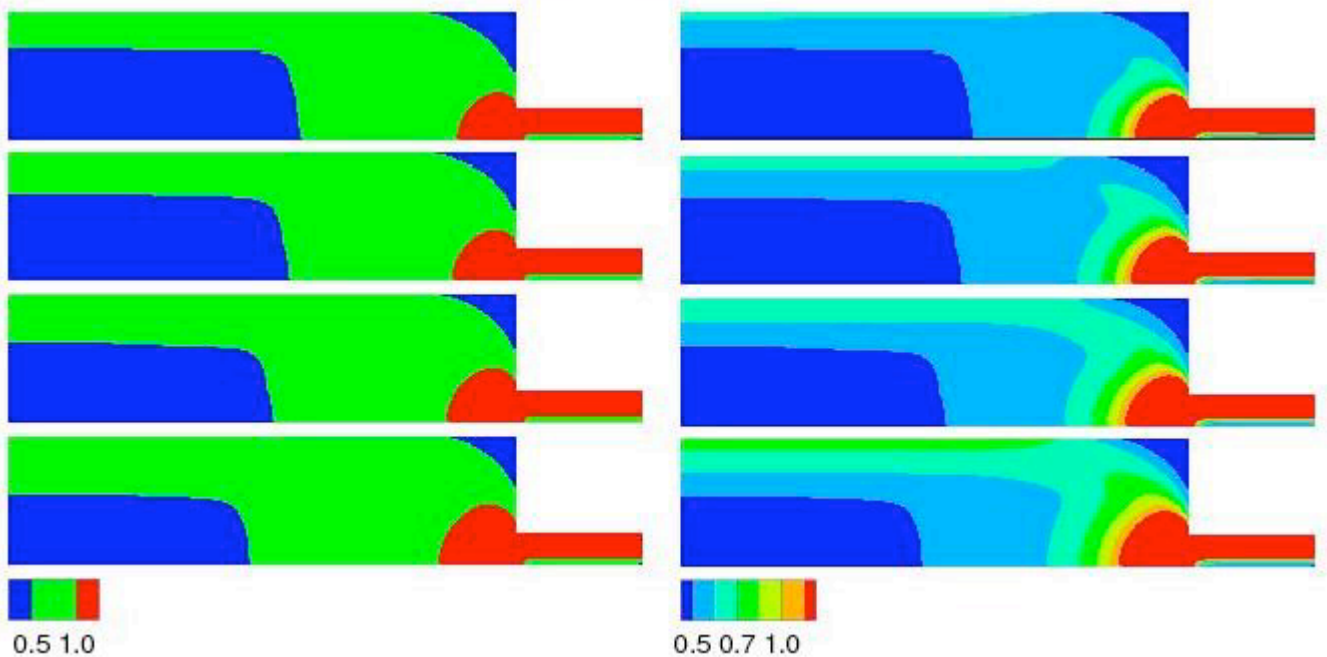
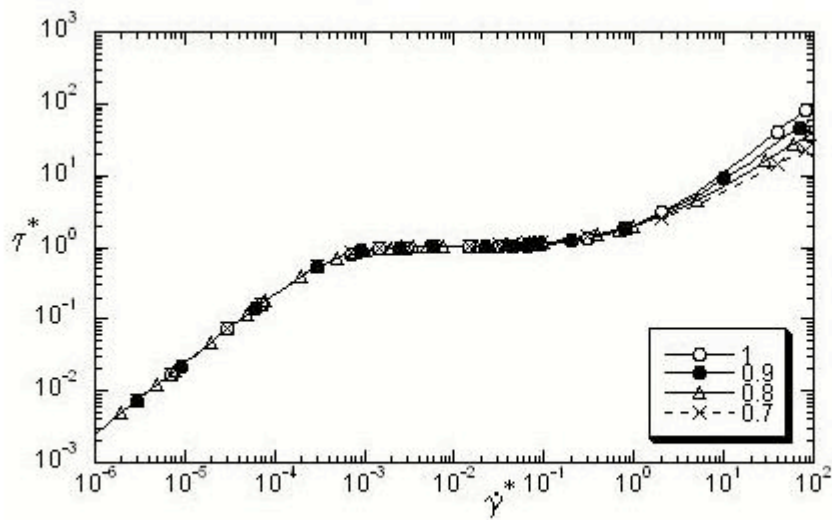


Figure 4. Stress intensity for a fixed value of the Jump Number, $J = 2500$, and different values of power-law index.

On the top of Fig. 5 is the same plot of the stress intensity as a function of the deformation rate for a fixed Jump number, $J = 2500$, and different values of the power-law index. The fields of the deformation rate for the different values the power-law index are shown below. On the left, there are only three levels of intensity: below $\dot{\gamma}_0$, between $\dot{\gamma}_0$ and $\dot{\gamma}_1$, and above $\dot{\gamma}_1$.

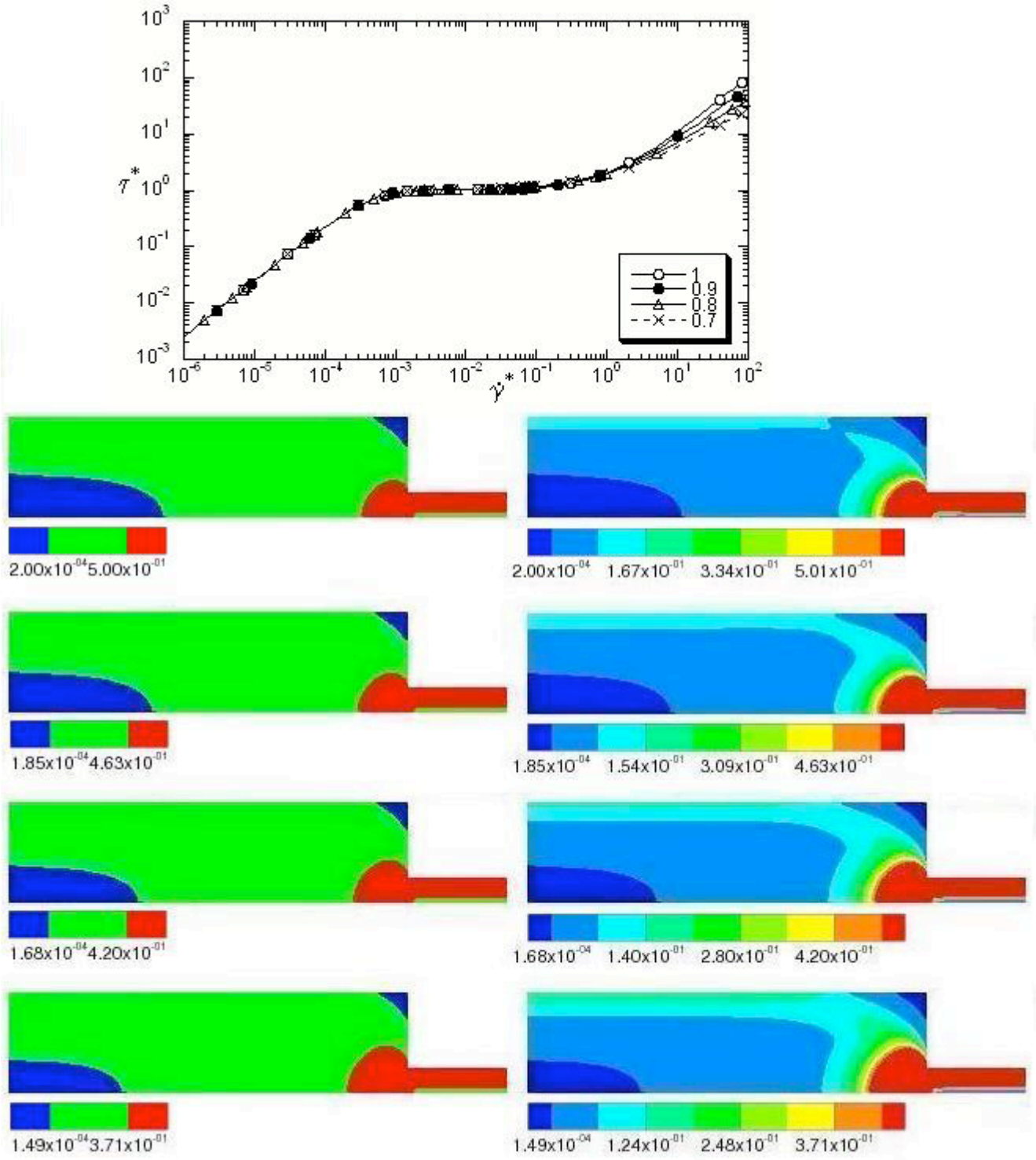


Figure 5. Deformation rate for a fixed value of the Jump Number, $J = 2500$, and different values of power-law index.

It can be seen that, for this level of the Jump number, the variation of the power-law index does not affect significantly the fields of stress intensity and deformation rate. The reason for this to happens is because the stress intensity as a

function of the deformation rate is only affected in its power-law region, at very high deformation rates, as shown on the top of Fig.5.

Figure 6 shows the field of deformation for different values of the Jump number. Here we can see that the dimensionless quantity has a strong influence on the field. The increase of J increases the portion of the field which is between $\dot{\gamma}_0$ and $\dot{\gamma}_1$. This change is accompanied by a decrease in the region of deformation rates below $\dot{\gamma}_0$, while the region above $\dot{\gamma}_1$ becomes unaltered.

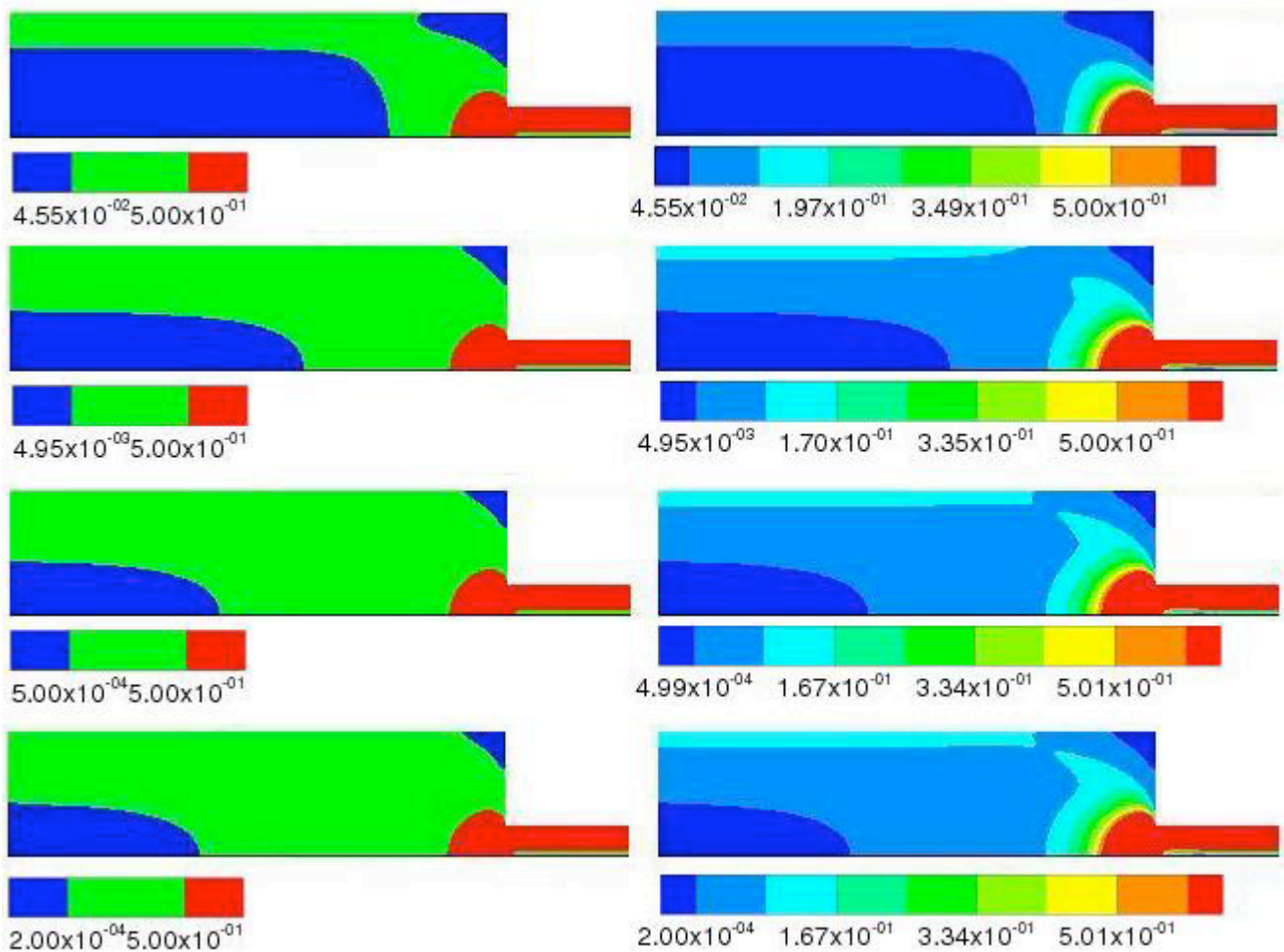


Figure 6. Deformation rate for different value of the Jump number, $J = 10, 100, 1000,$ and 2500 .

The Couette correction, a dimensionless number defined as the ratio of the pressure loss in the contraction and two times the stress at the wall of the small tube is given in Fig. 7.

5. FINAL REMARKS

The present work analyzes the SMD equation, conceived to model viscoplastic behavior, in a 4:1 abrupt contraction from the numerical point of view using a Glerkin/Finite Element method. The objective of the investigation is to study the influence of the Jump number and the power-law exponent of the model on the size and shape of the yield zone. The yield zone, in contrast to the yield surface, is a region of the domain where stresses are close to the apparent yield stress. In this region, there can be a large range of deformation rate, depending on the value of the Jump number.

In the range analyzed, namely $0.7 \leq n \leq 1$, the power-law index had a timid influence on the general results. The variation of the Jump number has a strong influence on the size of the yield zone, but does not affect significantly the Couette-correction.

6. ACKNOWLEDGEMENTS

This research was funded by grants from PETROBRAS, ANP (Petroleum National Agency), and CNPq (the Brazilian Research Council).

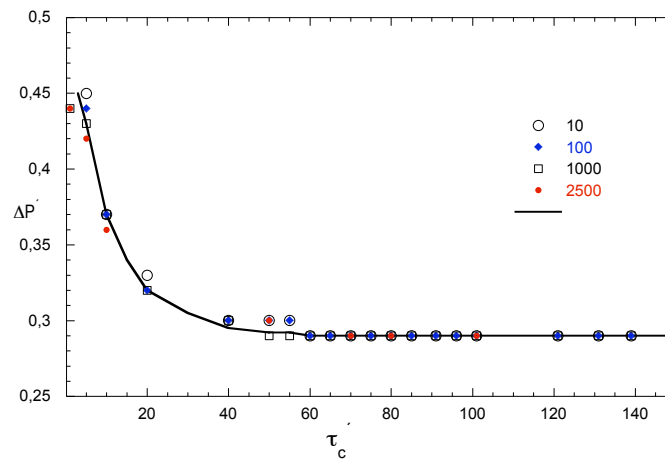


Figure 7. Pressure loss as a function of τ_c for different values of the Jump number.

7. REFERENCES

- Barnes, H., 1999. The yield stress, a review. *J. Non-Newt. Fluid Mech.* 81, 133–178.
- Bingham, E., 1922. *Fluidity and plasticity*. McGraw-Hill, Boston.
- de Souza Mendes, P., 2007. Dimensionless non-newtonian fluid mechanics. *J. Non-Newt. Fluid Mech.* 147, 109–116.
- de Souza Mendes, P., Dutra, E., 2005. Viscosity function for yield stress fluids. *Appl. Rheol.* 525, 1–26.
- Dimakopoulos, Y., Tsamopoulos, J., 2003. Transient displacement of a viscoplastic material by air in straight and suddenly constricted tubes. *J. Non-Newt. Fluid Mech.* 112, 43–75.
- Papanastasiou, T., 1987. Flows of materials with yield. *J. Rheol.* 81, 385–404.
- Sousa, D., Soares, E., Queiroz, R., Thompson, R., 2007. Numerical investigation on gas-displacement of a shear-thinning fluid and a visco-plastic material in capillary tubes. *J. Non-Newt. Fluid Mech.* 144, 149–159.
- You, Z., Huilgol, R., Mitsoulis, E., 2008. Application of the lambert w function to steady shearing flows of the papanastasiou model. *Int. J. Eng. Sci.* 46, 799–808.

8. Responsibility notice

The author(s) is (are) the only responsible for the printed material included in this paper